Multiple Sclerosis and Related Disorders 103 (2025) 106661

Contents lists available at ScienceDirect

Multiple Sclerosis and Related Disorders

journal homepage: www.elsevier.com/locate/msard

Original article

The early effect of induction versus continuous therapies in active multiple sclerosis: a multimodal study on the first course of cladribine versus fingolimod

Tommaso Sirito [a], Emilio Cipriano [a], Caterina Lapucci [b], Vincenzo Daniele Boccia [a], Ivan Panzera [c], Antonio Uccelli [a,b], Elisabetta Capello [b], Maria Cellerino [a], Matilde Inglese [a,b,*], Giacomo Boffa [a,b]

[a] Department of Neuroscience, Rehabilitation, Ophthalmology, Genetics, Maternal and Child Health (DiNOGMI), University of Genoa, Genoa, Italy
[b] IRCCS Ospedale Policlinico San Martino, Genoa, Italy
[c] Department of Neuroscience, Multiple Sclerosis Center- Neurology Unit, S.Maria delle Croci Hospital, Ravenna, Italy

ARTICLE INFO

Keywords:
Multiple sclerosis
Cladribine
Fingolimod
S1PR
Advanced biomarkers
Induction therapies

ABSTRACT

Background: Induction therapies for multiple sclerosis (MS), such as cladribine (CLAD), require multiple cycles to achieve full clinical effects, and the extent of immunosuppression from a single course is unclear. Fingolimod (FINGO), administered daily, provides a rapid anti-inflammatory effect, desirable for active MS.
Objectives: to compare the efficacy of the first course of CLAD versus FINGO over 12 months by analyzing clinical data, brain atrophy, retinal thinning, and diffusion MRI metrics of myelin and neuroaxonal integrity in the corpus callosum.
Methods: evaluations included NEDA-3 status, percentage brain volume change (PBVC) and changes in retinal nerve fibers and MRI metrics of the corpus callosum such as Intra-Cellular Volume Fraction (ICVF) and Orientation Dispersion Index (ODI).
Results: we included 65 relapsing-remitting MS patients (33 on CLAD, 32 on FINGO). After 12 months, 81.8% of CLAD patients and 71.9% of FINGO patients achieved NEDA-3 ($p = 0.4$). PBVC <-0.4% was observed in 41.9% of CLAD and 39.2% of FINGO patients ($p = 0.9$). Both drugs showed similar effects on retinal thinning and ICVF and ODI of the corpus callosum.
Conclusions: A single course of cladribine has comparable efficacy to daily fingolimod treatment based on clinical, OCT and advanced MRI measures.

1. Introduction

Most multiple sclerosis (MS) disease modifying treatments (DMTs) require continuous chronic administration to maintain their efficacy. Continuous administration ensures long-term immunomodulation, aligning with the clinical effectiveness of the drug. Upon discontinuation of therapy, disease activity may resume, and in some cases, disease rebound occurs. There is a class of drugs, known as 'immune reconstitution therapies' or 'immune depletion and repopulation therapies,' which are administered intermittently to induce short, transient periods of immunosuppression, potentially leading to the reconstitution of a more tolerant immune system (Sorensen and Sellebjerg, 2019) (Lünemann et al., 2020). This approach aims to provide disease control extending beyond the treatment period itself.

Both therapeutic strategies have distinct advantages and disadvantages. Continuous administration therapies have substantial long-term efficacy data (Cohen et al., 2019), whereas there is limited information on the long-term efficacy of induction therapies beyond five years. Induction therapies require multiple cycles to achieve full clinical effect, and the extent of immunosuppression obtained from a single cycle is not fully understood. Managing patients with disease activity between the first and second cycles remains uncertain, potentially exposing patients to relapse risks (Sørensen et al., 2020). On the contrary, continuous administration, especially of newer high-efficacy immunosuppressive

* Corresponding author at: Department of Neuroscience, Rehabilitation, Ophthalmology, Genetics, Maternal and Child Health (DiNOGMI), University of Genoa, Genoa, Italy, Largo Paolo Daneo3, Genova 16100, Italy.
E-mail address: m.inglese@unige.it (M. Inglese).

https://doi.org/10.1016/j.msard.2025.106661
Received 1 October 2024; Received in revised form 22 January 2025; Accepted 30 July 2025
Available online 9 August 2025
2211-0348/© 2025 The Authors. Published by Elsevier B.V. This is an open access article under the CC BY license (http://creativecommons.org/licenses/by/4.0/).

drugs, may result in severe complications, including increased infectious and oncogenic risks (Langer-Gould et al., 2023), while the immunosuppression following induction therapies is brief and easily monitored.

Fingolimod and cladribine represent two of the most used drugs within the continuous and induction therapy categories, respectively. Both are oral medications, indicated for patients with active MS, and appear to have comparable efficacy profiles (Signori et al., 2020). Lymphocyte depletion after cladribine is slower and milder compared to fingolimod, which may be a limiting factor when aiming for a rapidly effective anti-inflammatory effect, even though it is not clear whether the kinetics of immune depletion mirror the onset of the clinical efficacy (Comi et al., 2019). Cladribine requires two treatment cycles to fully exert its effectiveness; therefore, the possibility of disease relapse between the first and second cycles can alert the prescribing neurologist. Recently, it has been suggested that a single cycle of cladribine may provide the same level of disease control as continuous fingolimod (Brownlee et al., 2023). However, this study considered only standard clinical and radiological data, limiting the information on the true short-term efficacy of the two drugs and preventing a real comparison of the speed of action between the two treatments. Quantitative measures of walking speed, manual dexterity and balance can improve our ability to monitor DMT efficacy. Moreover, a more comprehensive evaluation of the inflammatory and degenerative mechanisms of MS, including the analysis of brain and retinal nerve atrophy and the microstructural damage occurring in normal appearing white matter are useful to elucidate the role of modern DMTs.

Against this background, the aim of this study was to investigate through a multimodal approach, the efficacy of the first course of cladribine versus fingolimod over the first 12 months from treatment start analysing clinical data, brain atrophy rates, changes in diffusion MRI metrics of myelin and neuroaxonal integrity of the corpus callosum and the atrophy rates of peripapillary retinal nerve fiber (pRNFL), and ganglion cell + inner plexiform layers (GCIPL) as assessed with optical coherence tomography (OCT).

2. Methods

2.1. Subjects

This is a prospective, longitudinal, real-world study. Sixty-five consecutive patients who were prescribed treatment with either fingolimod ($n = 32$) or cladribine ($n = 33$) were enrolled. All subjects gave their written informed consent to participate in the study, which was approved by the local ethics committee. The patients' identities were anonymized for the analyses. Inclusion criteria were: (i) age 10–70 years (ii) MS diagnosis according to the 2017 McDonald's criteria (Thompson et al., 2018). Exclusion criteria were: (i) contraindications to MRI, (ii) progressive disease course according to Lublin's criteria (Lublin et al., 2014). Patients were clinically evaluated every 3 months for assessment of effectiveness and safety. Sixty-four (98 %) underwent baseline and 12-months follow-up (FU) MRI scans at our institution with a standardized 3T MRI protocol (Siemens PRISMA). A subset of patients ($n = 53$) underwent spectral domain optical coherence tomography (SD-OCT) at the same timepoints.

2.2. Clinical assessment

Clinical evaluation included (a) assessment of Extended Disability Status Scale (EDSS) score (Kurtzke, 1983); (b) Nine-Hole Peg Test (9-HPT) (Feys et al., 2017); (c) Timed 25-foot walk test (Kalinowski et al., 2022); and (d) NIH Toolbox Standing Balance Test (Peller et al., 2023). The NIH Toolbox Standing Balance Test is a tool that assesses balance maintenance in five positions: with open and closed eyes on solid and soft surfaces and with open eyes in a tandem position on a solid surface. A coefficient is calculated based on the patient's balance during each position; the average of the 5 coefficients, known as the theta value (ranging from −2 to +2, where a lower value indicates less balance in the patient), is a reliable and validated estimate of the patient's balance. Information regarding occurrence of clinical relapses and/or disability progression during FU were collected.

2.3. MRI acquisition

MRI exam was performed using a 3-T Siemens MAGNETOM Prisma (Siemens Healthcare, Erlangen, Germany) scanner with a 64-channel head and neck coil. The MRI protocol included:

(i) 3D sagittal T2- FLAIR (repetition time/inversion time/echo time (TR/TI/TE): 5000 ms/1800 ms/393 ms; resolution 0.4 × 0.4 × 1 mm 3, acquisition time 6min37");
(ii) 3D sagittal T1 MPRAGE (TR/TI/TE: 2300 ms/919 ms/2.96 ms; resolution 1 × 1 × 1 mm 3, acquisition time 5min12");
(iii) twice-refocused spin echo-planar imaging sequence for diffusion MRI with 108 directions distributed in 5 shells with b-value up to 3000s/mm^2, in addition to seven $b = 0$ images (TR/TE: 4600/75 ms, flip angle 90°, spatial resolution 1.8 × 1.8 × 1.8 mm3, acquisition time 10min10"). Seven b = 0 image volumes with reversed phase-encoding direction were also acquired to correct for susceptibility-induced image distortions.

Of the 65 patients who underwent standardized 3-T MRI, 5 patients were excluded from the analyses of advanced resonance measurements due to: (I) treatment discontinuation within 6 months from treatment start ($n = 2$; 1 patient in the fingolimod and 1 in the cladribine group); (II) poor quality ($n = 3$, 2 patients in the fingolimod group and 1 in the cladribine group). Accordingly, MRI data were available for 31 patients treated with cladribine and for 29 fingolimod treated patients. Information regarding the presence of radiological disease activity (new/enlarging FLAIR lesions and gadolinium enhancing lesions) during FU was collected.

2.4. MRI processing

2.4.1. Lesion segmentation and brain atrophy

Lesions with T2 hyperintensity and T1 hypointensity were identified and delineated on FLAIR and T1-weighted images, respectively using a semi-automated segmentation technique based on user-guided local thresholding within a web-based platform (SinLab, SienaImaging, Siena, Italy; https://sinlab-rhb.sienaimaging.com). Subsequently, the corresponding T1 images were adjusted using the T1-hypointense lesion mask and the FMRIB Software Library (FSL) (Oxford, UK; https://fsl.fmrib.ox.ac.uk). Normalized brain, white matter (WM), and gray matter (GM) volumes were obtained through a fully automated segmentation pipeline (CAT12) (Gaser et al., 2022). To ensure quality, all segmentation maps have been checked manually. Changes in percentage-brain-volume- change (PBVC) were measured.

2.4.2. Diffusion processing

For diffusion MRI data, initial denoising was carried out using the Marchenko-Pastur principal component analysis algorithm available in Mrtrix3 (Tournier et al., 2019). Subsequently, corrections for motion artifacts and susceptibility-induced distortions were applied using the 'eddy' and 'top-up' commands from FSL. As a final pre-processing step, B1 field inhomogeneity correction was applied to all diffusion MRI volumes using the ANTs N4 algorithm.

The NODDI model was applied to extract the Intra-Cellular Volume Fraction (ICVF) and Orientation Dispersion (ODI) (Daducci et al., 2015). The first measures the volume occupied by cellular structures in brain tissue. The second quantifies the dispersion of neural fiber orientations in a brain region, indicating how fibers align or spread (Sacco et al., 2020).

The Corpus Callosum (CC) region of interest (ROI) for the was

extracted from the JHU atlas (MRI Atlas of Human White Matter 2020): a non-linear transformation (Symmetric normalization, which combines an Affine and deformable transformation) was used to register the T2 image based on JHU template onto the mean $b = 0$ vol extracted from the dMRI images (Avants et al., 2011). Then the resulting transformations were applied to register the CC ROI within the dMRI space. Moreover, the coregistered CC mask was eroded by one voxel to avoid Partial Volume Effect (PVE) with neighboring tissue. All the registrations underwent visual inspection for quality assurance. Finally, the mean values of diffusion microstructural maps were extracted within the CC mask.

2.5. OCT

Standardized spectral-domain-OCT protocols (Spectralis, Heidelberg-Engineering) were performed and processed by a single certified neurologist, in accordance with the APOSTEL recommendations (Cruz-Herranz et al., 2016). Peripapillary retinal nerve fiber layer (pRNFL) was obtained with a 360° RNFL-B circle scan located at 3.4 cm from the center of the optic nerve head; peripapillary measurements were averaged from 100 images and macular estimations from 15 ART. Macular volumetric scans consisting of at least 25 single horizontal axial B-scans were acquired in a rectangular section centered over the macula and segmented automatically into different layers using the Heidelberg Eye Explorer mapping software version 6.0.9.0. Segmented layers were checked and manually corrected, if necessary. The combined thickness of ganglion cell layer + inner plexiform layer (GCIPL) was measured.

Table 1
Baseline clinical and demographic characteristics of the study groups.

	Patients treated with CLAD	Patients treated with FINGO	P value
Nr, of patient (%)	33 (50.76 %)	32 (49.23 %)	–
Age, mean (SD)	39.42 (± 11.34)	40.13 (± 16.72)	0.84
Female, number (%)	22 (66.66 %)	20 (62.5 %)	0.72
Disease duration, years, mean (SD)	7.66 (± 9.15)	9.4 (± 10.05)	0.46
EDSS, median (range)	1.5 (0–4.5)	1.5 (0–5.5)	0.32
ARR in the previous year, mean (range)	0.30 (± 0.64)	0.16 (± 0.37)	0.37
Naïve patients, (%)	15 (45.45 %)	15 (46.88.12 %)	1
Previous DMT:	5 (27.78 %)	6 (35.28 %)	
dimethylfumarate	4 (22.22 %)	0	
S1P receptor modulators	3 (16.67 %)	5 (29.41 %)	
glatiramer acetate	3 (16.67 %)	2 (11.76 %)	
interferon	2 (11.11 %)	3 (17.65 %)	
teriflunomide	1 (5.56 %)	1 (5.88 %)	
natalizumab			
Reason for switching from previous DMT:	7 (38.89 %)	14 (82.32 %)	
inefficacy	7 (38.89 %)	1 (5.88 %)	
intollerance	4 (22.22 %)	0	
safety	0	2 (11.76 %)	
others			
Previous DMTs, number, median (range)	1.5 (0–5.5)	1 (0–3)	0.57
Disease activity on baseline MRI, number (%)	13 (39.39 %)	20 (62.5 %)	0.06
Baseline total brain volume MRI, ml, mean (SD)	1400.90 (± 134.80)	1396.33 (± 149.04)	0.77
T2 Lesion load at baseline MRI, ml, mean (SD)	8.95 (± 11.50)	12 (± 16.28)	0.57
Baseline pRNFL, µm, mean (SD)	100.70 (±9.71)	98.10(±11.10)	0.54
Baseline GCIPL, µm, mean (SD)	86.10 (±4.79)	83.20 (±10.20)	0.52

CLAD = cladribrine; FINGO = fingolimod; EDSS= Expanded Disability Status Scale; ARR= annualized relapse rate; DMTs= Disease Modifying Therapies; MRI= magnetic resonance imaging; pRNFL= peripapillary retinal nerve fiber layer; GCIPL= ganglion cell layer + inner plexiform layer; SD= standard deviation.

Scans violating international-consensus quality-control criteria (OSCAR-IB) (Schippling et al., 2015) were excluded ($n = 8$ fingolimod treated and $n = 6$ cladribine treated patients excluded due to poor OCT quality). Patients with previous bilateral optic neuritis (ON) were excluded ($n = 4$). In patients with previous unilateral ON ($n = 44$, none occurring during the previous 12-months), only the non-affected eye was analyzed. In patients without history of ON, OCT metrics were averaged over the two eyes.

2.6. Study end points

The endpoints of our study were to compare the: I) percentage of patients free from clinical relapses, MRI activity and disability progression (according to the NEDA-3 definition) during the first 12 months after treatment start; II) changes in 9-HPT, T25-foot walk, and theta value at NIH Toolbox Standing Balance Test scores; (III) percentage of patients maintaining NEDA-4 (NEDA-3 plus absence of pathological brain atrophy, defined as an annualized PBVC>−0.4 % (De Stefano et al., 2015)); (IV) retinal (pRNFL and GCIPL) atrophy; (V) changes in NODDI metrics (ODI and ICVF) within the corpus callosum.

2.7. Statistical analysis

Statistical analyses were performed with SPSS (v26.0) and Jamovi (v 2.5.2.0). Descriptive results were reported as mean with standard deviation (SD) or median with interquartile range (IQR). Demographic differences between groups were analyzed using Chi-square, Mann-Whitney and Student's *t*-test when appropriate. The probability of disability worsening-free survival, relapse-free survival, MRI activity-free survival, and NEDA-3 status was calculated with the Kaplan–Meier estimator. Differences in terms of clinical (9-HPT, T25-foot walk and theta value at NIH Toolbox balance standing test scores), MRI (T2 lesion load, ODI and ICVF of CC) and OCT (pRNFL and GCIPL) metrics at different timepoints were assessed with repeated-measure analysis of covariance, adjusting for age, sex, and disease duration. A two-sided $p < 0.05$ was used for statistical significance.

3. Results

3.1. Study population

Table 1 reports main demographic and disease related characteristics of the two groups. Patients were well balanced for main baseline characteristics. Mean age at baseline was 39.4 (± 11.3) years in the cladribine-treated group (CLAD) and 40.1 years (± 16.7) in the fingolimod-treated group (FINGO), with 66.7 % and 62.5 % of females,

Table 2
Clinical outcomes.

	Patients treated with CLAD	Patients treated with FINGO	P value
Progression free survival, nr (%)	33 (100 %)	32 (96.9 %)	0.31
Relapse free survival, nr (%)	31 (93.93 %)	32 (100 %)	0.16
MRI activity free survival, number (%)	27 (81.8 %)	24 (75 %)	0.56
Maintenance of NEDA3, nr (%)	27 (81.8 %)	23 (71.9 %)	0.41
Mean difference at 9-HPT test, seconds (SD)	−0.51 (±3.08)	+1.21(±3.66)	0.11
Mean difference of theta value at NIH Toolbox Standing Balance test (SD)	−0.3(±0.8)	−0.1 (±0.8)	0.74
Mean difference at T25FW test, seconds (SD)	+0.45(±3.21)	+1.07 (±3.17)	0.23

CLAD = cladribrine; FINGO = fingolimod; MRI= magnetic resonance imaging; NEDA= non evidence of disease activity; 9HPT:Nine-Hole Peg Test; T25FW=timed 25 foot walk;; SD=standard deviation.

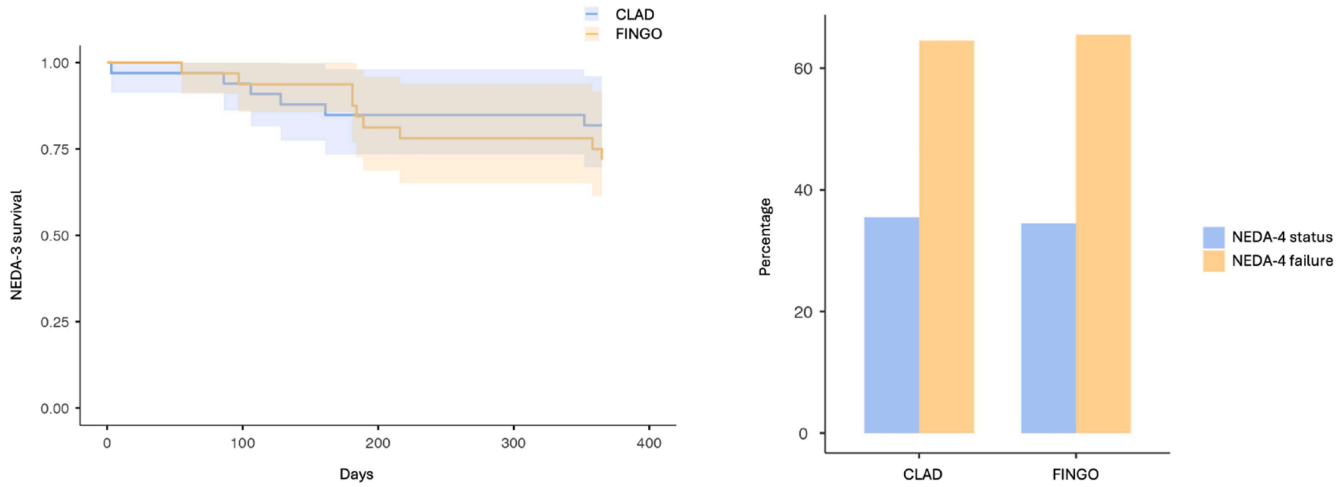

Fig. 1. NEDA-3 and NEDA-4 probabilities NEDA= No evidence of disease activity. NEDA-3 status is defined as the absence of relapses, new activity on brain MRI, and disability progression. NEDA-4 meets all NEDA-3 criteria plus lack of brain atrophy.

Table 3
MRI and OCT outcomes.

	Patients treated with CLAD	Patients treated with FINGO	P value
Number of patients with PBVC <0.4 %, nr (%)	13 (41.93 %)	11 (37.93 %)	0.75
Maintenance of NEDA4, nr (%)	11 (35.48 %)	10 (34.48 %)	0.93
Mean difference in ICVF value in the corpus callosum (SD)	+0.003 (±0.01)	+0.003 (±0.02)	0.21
Mean difference in ODI value in the corpus callosum (SD)	+0.002 (±0.01)	+0.002 (±0.02)	0.88
Mean difference in pRFNL, μm (SD)	−1.6(±3.2)	−1.3(±1.7)	0.31
Mean difference in GCIPL, μm (SD)	−1.6(±2.5)	−0.7(± 2.0)	0.32

CLAD = cladribrine; FINGO = fingolimod; PBVC=Percentage brain volume change; NEDA= non evidence of disease activity; ICVF=Intra-Cellular Volume Fraction; ODI= Orientation Dispersion; pRNFL= peripapillary retinal nerve fiber layer; GCIPL= ganglion cell layer + inner plexiform layer; SD=standard deviation.

respectively. Mean disease duration was 7.7 (± 9.2) and 9.4 (±10) years for CLAD and FINGO respectively, with a median EDSS at baseline of 1.5 (0–4.5 for CLAD group and 0–5.5 for FINGO group) for both groups. Fifteen patients per cohort (30 in total), that is, 45.45 % in the CLAD group and 46.88 % in the FINGO group, were treatment-naïve. 39.4 % of patients who initiated CLAD had MRI activity at baseline vs 62.5 % of those who initiated FINGO ($p = 0.06$).

3.2. Clinical outcomes

Table 2 shows the main clinical outcomes. After 12 months, 81.8 % of CLAD patients obtained NEDA-3 status compared to 71.9 % of FINGO patients ($p = 0.41$). Only one patient treated with fingolimod had disability progression, which was independent of relapse activity. The percentage of patients free of relapse activity was 93.9 % and 100 %, for CLAD and FINGO respectively. Two patients relapsed under CLAD (one had a relapse 3 days after the start of therapy -with subsequent persistent MRI activity-, while the other relapsed after 258 days). 81.8 % of CLAD patients was free of MRI activity versus 75 %, in the FINGO group. Mean time to MRI activity was 160 days and 229 days, respectively. Kaplan-Meier figures related to NEDA-3 loss are depicted in Fig. 1.

CLAD patients exhibited a minimal increase of 0.45 s (± 3.21) in T25FW compared to 1.07 (± 3.17) seconds for the FINGO group. Similarly, both groups demonstrated a slight reduction of 0.3 (± 0.8) and 0.1 (± 0.8) in the theta value at the NIH Toolbox Standing Balance Test over 12 months. Regarding 9-HPT, we observed a reduction of 0.51 s (± 3.08) in CLAD patients and an increase of 1.21 s (± 3.66) in FINGO patients. These longitudinal changes were not statistically significant and did not differ between study groups.

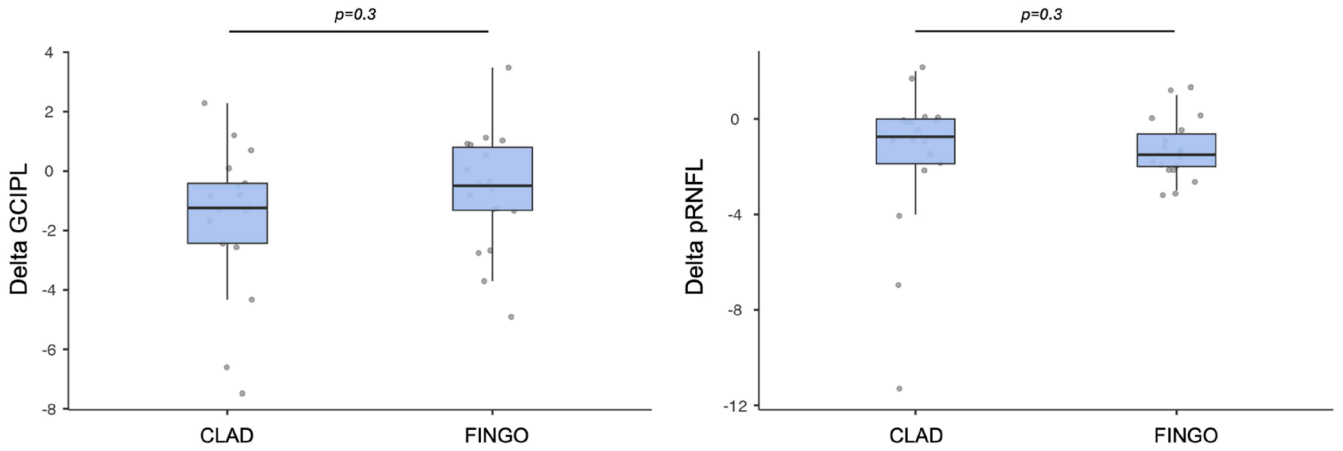

Fig. 2. OCT metrics changes pRNFL= peripapillary retinal nerve fiber; GCIPL= ganglion cell + inner plexiform layers.

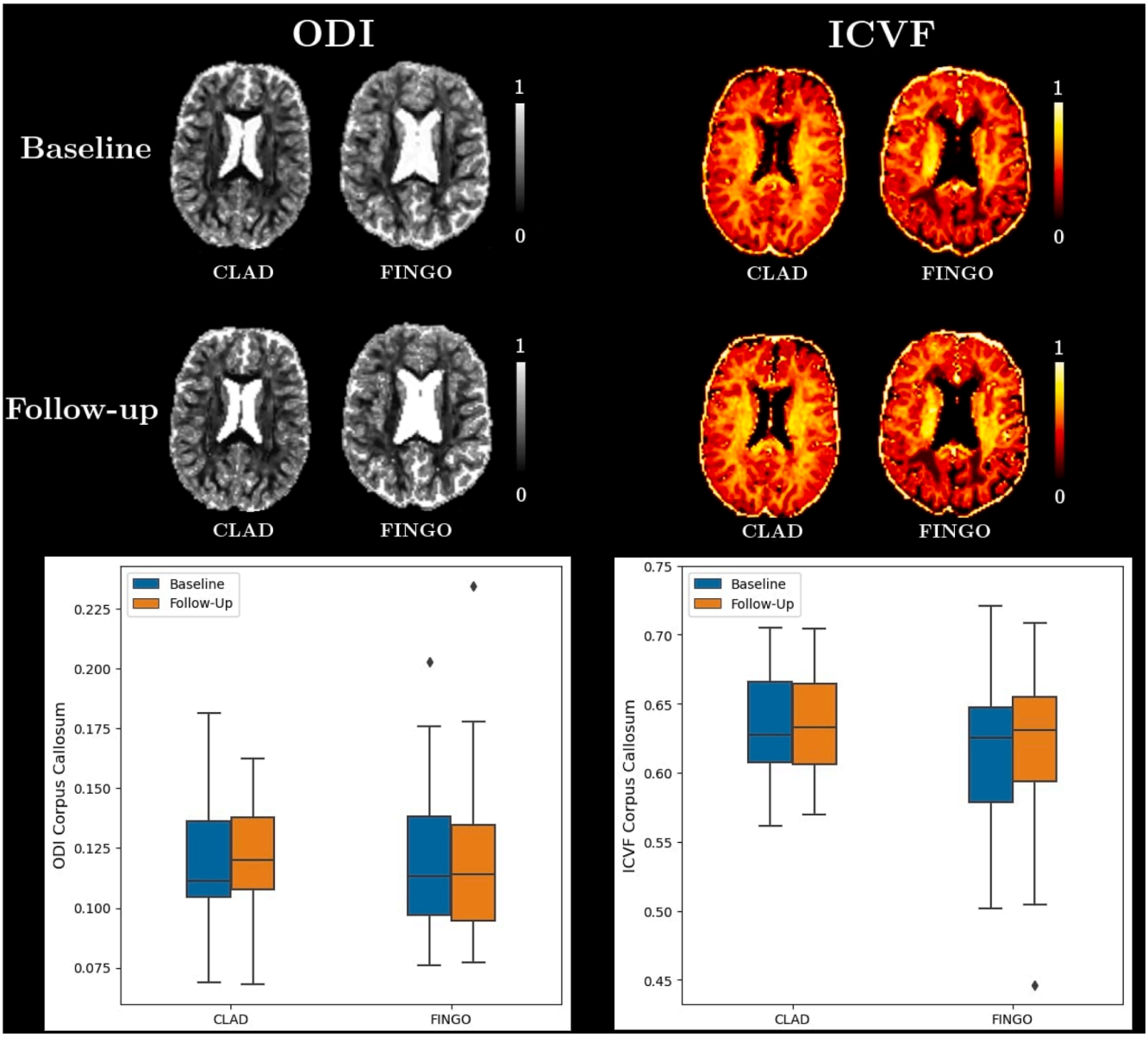

Fig. 3. NODDI microstructural changes within the corpus callosum ODI= Orientation Dispersion Index. ODI quantifies the dispersion of neural fiber orientations in a brain region, indicating how fibers align or spread; ICVF= Intra-Cellular Volume Fraction. ICVF measures the volume occupied by cellular structures in brain tissue.

3.3. Brain volumes and NEDA-4 status

The percentage of patients with PBVC <−0.4 % was 41.9 % (13 patients) and 37.9 % (11 patients), respectively. The number of patients who maintained NEDA-4 at 12 months was 11 for CLAD patients and 10 for FINGO patients (Fig. 1 and Table 3).

3.4. OCT

Retinal thinning over FU was similar between patients treated with cladribine (pRNFL: −1.6 ± 3.2 μm; GCIPL: −1.6 ± 2.5 μm) and fingolimod (pRNFL: −1.3 ± 1.7 μm; GCIPL: −0.71 ± 2 μm; Table 3). Fig. 2 reports the delta of GCIPL and pRNFL over 12 months of the two treatment groups.

3.5. Microstructural integrity of the corpus callosum

We observed a substantial stability ICVF and ODI measures within the corpus callosum; ICVF increased by 0.003 in both groups, while ODI increased by 0.002 in both groups. Fig. 3 reports representative ICVF and ODI maps from 2 patients, with the mean values within the corpus callosum of the study groups at baseline and after 12 months.

3.6. Persistence on therapy and adverse events

29/33 (87 %) of CLAD patients did not discontinue therapy versus 30/32 (93 %) of FINGO patients. For CLAD patients, therapeutic switch occurred in 3 cases due to lack of efficacy, and in one case due to the detection, shortly before starting the second cycle of cladribine, of thyroid carcinoma, for which the patient was switched to natalizumab. 2 patients discontinued fingolimod due to lack of efficacy. No additional adverse events related to the two drugs were observed.

4. Discussion

In this study, we provide evidence of the early effectiveness of cladribine and fingolimod in a real-life population of MS patients. Our data confirm and extend previous works, indicating that one course of

cladribine has a comparable clinical efficacy with daily treatment with fingolimod. 82 % of cladribine treated patients and 72 % of fingolimod treated patients achieved complete disease control according to the NEDA-3 definition, with only 2 relapses occurring in the CLAD group over the first 12 months. Of interest, no differences were noted in quantitative clinical measures of manual dexterity, walking speed and balance between the two study groups, with an overall stabilization of all parameters. Incorporating brain atrophy as an outcome measure, we found that 35.5 % of CLAD patients and 34.5 % of FINGO patients achieved NEDA-4 status over the first 12 months. These results are encouraging considering that, since no re-baseline MRI was performed in this study, some patients with pathologic brain atrophy (<−0.4 % of percentage brain volume change) might have experienced a pseudoatrophy effect (De Stefano and Arnold, 2015), consisting in a reduction of brain volume due to oedema resolution. To this regard, it is interestingly to note that one course of cladribine was equivalent to continuous fingolimod in controlling the retinal thinning assessed by OCT, which has been associated to neurodegeneration and brain volume loss (Gordon-Lipkin et al., 2007). Altogether these results suggest that cladribine and fingolimod are able to induce a rapid control of the inflammatory activity in active MS patients, with a potential neuroprotective effect.

We also analyzed the early effect of the DMTs on the microstructural properties of the corpus callosum, which has proposed as a biomarker for reparative studies (Caverzasi et al., 2023). Using NODDI, an advanced diffusion MRI model, we found an overall stabilization of ODI and ICVF, two metrics reflecting the organization and the volume of neurons and oligodendrocytes in the WM. Again, these results suggest that one course of cladribine is equivalent to continuous fingolimod treatment in preserving WM microstructural integrity in MS patients.

The multimodal approach adopted in this study allows for the simultaneous evaluation of various critical aspects of DMTs for MS, including the speed of action, the intensity of their immunosuppressive effects, and their ability to mitigate neuronal damage. We have demonstrated that a single course of an inductive oral therapy exerts similar effects on MS pathology in terms of rapidity and intensity as a continuous sequestering agent.

The primary limitation of this study is its uncontrolled design and small sample size. Despite the well-balanced clinical and MRI characteristics and demographics between the two patient groups, the slightly higher proportion of inflammatory MRI activity in fingolimod-treated patients prior to treatment initiation could have influenced the slightly lower rates of NEDA-4 in this group. While the small sample size may limit the generalizability of our clinical results, they are consistent with larger real-world experiences.

Ethics approval and consent to participate

All subjects gave their written informed consent to participate in the study, which was approved by the local ethics committee (CER Liguria 74/2020).

Consent for publication

All authors have read the manuscript and agree with its contents. We have full access to the data and the right to publish them apart from any sponsor. We take full responsibility for the data, the analyses and interpretation, and the conduct of the research.

Funding statement

The work was supported by grants from Italian Ministry of Health, Ministero della Salute (Ricerca Corrente RRC 2022 and 5 × 1000) and by NextGenerationEU funded by the Italian Ministry of University and Research, National Recovery and Resilience Plan, project MNESYS (PE0000006).

Availability of data and material

The data that support the findings of this study are available from the corresponding author upon request.

Funding statement

The work was supported by grants from Italian Ministry of Health, Ministero della Salute (Ricerca Corrente RRC 2022 and 5×1000) and by NextGenerationEU funded by the Italian Ministry of University and Research, National Recovery and Resilience Plan, project MNESYS (PE0000006).

CRediT authorship contribution statement

Tommaso Sirito: Methodology, Writing – original draft, Formal analysis, Investigation, Data curation. **Emilio Cipriano:** Visualization, Methodology, Data curation, Software, Investigation, Conceptualization. **Caterina Lapucci:** Validation, Visualization, Supervision. **Vincenzo Daniele Boccia:** Data curation, Formal analysis. **Ivan Panzera:** Investigation, Data curation, Formal analysis. **Antonio Uccelli:** Validation, Supervision. **Elisabetta Capello:** Validation, Supervision. **Maria Cellerino:** Investigation, Conceptualization, Supervision, Formal analysis, Methodology, Data curation. **Matilde Inglese:** Supervision, Visualization, Validation. **Giacomo Boffa:** Supervision, Investigation, Conceptualization, Visualization, Software, Formal analysis, Validation, Methodology, Data curation.

Declaration of competing interest

GB received personal compensations from Novartis, Sanofi Genzyme, Roche, BMS and Merck. CL received travel grants from Roche, Merck, Sanofi and honoraria for speaking from Novartis, Roche, Merck, Horizon and BMS. MC received personal compensations from Novartis, Sanofi Genzyme, Teva and consulting fees from Zambon. MI received grants NIH, NMSS, FISM; received fees for consultation from BMS; Janssen, Roche, Genzyme, Merck, Biogen and Novartis. None of these personal compensations were related to this work. TS, AU, VDB, EC, IP and EC have nothing to disclose.

References

Sorensen, P.S., Sellebjerg, F., 2019. Pulsed immune reconstitution therapy in multiple sclerosis. Ther. Adv. Neurol. Disord. 12, 175628641983691. https://doi.org/10.1177/1756286419836913.

Lünemann, J.D., Ruck, T., Muraro, P.A., Bar-Or, A., Wiendl, H., 2020. Immune reconstitution therapies: concepts for durable remission in multiple sclerosis. Nat. Rev. Neurol. 16 (1), 56–62. https://doi.org/10.1038/s41582-019-0268-z.

Cohen, J.A., Tenenbaum, N., Bhatt, A., Zhang, Y., Kappos, L., 2019. Extended treatment with fingolimod for relapsing multiple sclerosis: the 14-year LONGTERMS study results. Ther. Adv. Neurol. Disord. 12, 175628641987832. https://doi.org/10.1177/1756286419878324.

Sørensen, P.S., Centonze, D., Giovannoni, G., et al., 2020. Expert opinion on the use of cladribine tablets in clinical practice. Ther. Adv. Neurol. Disord. 13, 175628642093501. https://doi.org/10.1177/1756286420935019.

Langer-Gould, A.M., Smith, J.B., Gonzales, E.G., Piehl, F., Li, B.H., 2023. Multiple sclerosis, disease-modifying therapies, and infections. Neurol. Neuroimmunol. Neuroinflammation 10 (6), e200164. https://doi.org/10.1212/NXI.0000000000200164.

Signori, A., Saccà, F., Lanzillo, R., et al., 2020. Cladribine vs other drugs in MS: merging randomized trial with real-life data. Neurol. Neuroimmunol. Neuroinflammation 7 (6), e878. https://doi.org/10.1212/NXI.0000000000000878.

Comi, G., Cook, S., Giovannoni, G., et al., 2019. Effect of cladribine tablets on lymphocyte reduction and repopulation dynamics in patients with relapsing multiple sclerosis. Mult. Scler. Relat. Disord. 29, 168–174. https://doi.org/10.1016/j.msard.2019.01.038.

Brownlee, W.J., Haghikia, A., Hayward, B., et al., 2023. Comparative effectiveness of cladribine tablets versus fingolimod in the treatment of highly active multiple sclerosis: a real-world study. Mult. Scler. Relat. Disord. 76, 104791. https://doi.org/10.1016/j.msard.2023.104791.

Thompson, A.J., Banwell, B.L., Barkhof, F., et al., 2018. Diagnosis of multiple sclerosis: 2017 revisions of the McDonald criteria. Lancet Neurol. 17 (2), 162–173. https://doi.org/10.1016/S1474-4422(17)30470-2.

Lublin, F.D., Reingold, S.C., Cohen, J.A., et al., 2014. Defining the clinical course of multiple sclerosis: the 2013 revisions. Neurology 83 (3), 278–286. https://doi.org/10.1212/WNL.0000000000000560.

Kurtzke, J.F., 1983. Rating neurologic impairment in multiple sclerosis: an expanded disability status scale (EDSS). Neurology 33 (11), 1444. https://doi.org/10.1212/WNL.33.11.1444. -1444.

Feys, P., Lamers, I., Francis, G., et al., 2017. The Nine-Hole Peg Test as a manual dexterity performance measure for multiple sclerosis. Mult. Scler. J. 23 (5), 711–720. https://doi.org/10.1177/1352458517690824.

Kalinowski, A., Cutter, G., Bozinov, N., et al., 2022. The timed 25-foot walk in a large cohort of multiple sclerosis patients. Mult. Scler. J. 28 (2), 289–299. https://doi.org/10.1177/13524585211017013.

Peller, A., Garib, R., Garbe, E., et al., 2023. Validity and reliability of the NIH toolbox® standing balance test as compared to the biodex balance system SD. Physiother. Theory Pract 39 (4), 827–833. https://doi.org/10.1080/09593985.2022.2027584.

Gaser, C., Dahnke, R., Thompson, P.M., Kurth, F., Luders, E., 2022. Alzheimer's disease neuroimaging initiative. CAT – A computational anatomy toolbox for the analysis of structural MRI data. Neuroscience. https://doi.org/10.1101/2022.06.11.495736.

Tournier, J.D., Smith, R., Raffelt, D., et al., 2019. MRtrix3: a fast, flexible and open software framework for medical image processing and visualisation. NeuroImage 202, 116137. https://doi.org/10.1016/j.neuroimage.2019.116137.

Daducci, A., Canales-Rodríguez, E.J., Zhang, H., Dyrby, T.B., Alexander, D.C., Thiran, J. P., 2015. Accelerated microstructure imaging via convex optimization (AMICO) from diffusion MRI data. NeuroImage 105, 32–44. https://doi.org/10.1016/j.neuroimage.2014.10.026.

Sacco, S., Caverzasi, E., Papinutto, N., et al., 2020. Neurite orientation dispersion and density imaging for assessing acute inflammation and lesion evolution in MS. Am. J. Neuroradiol. 41 (12), 2219–2226. https://doi.org/10.3174/ajnr.A6862.

MRI atlas of human white matter. AJNR Am. J. Neuroradiol. 27 (6), 2006, 1384–1385. PMCID: PMC8133945.

Avants, B.B., Tustison, N.J., Song, G., Cook, P.A., Klein, A., Gee, J.C., 2011. A reproducible evaluation of ANTs similarity metric performance in brain image registration. NeuroImage 54 (3), 2033–2044. https://doi.org/10.1016/j.neuroimage.2010.09.025.

Cruz-Herranz, A., Balk, L.J., Oberwahrenbrock, T., et al., 2016. The APOSTEL recommendations for reporting quantitative optical coherence tomography studies. Neurology 86 (24), 2303–2309. https://doi.org/10.1212/WNL.0000000000002774.

Schippling, S., Balk, L., Costello, F., et al., 2015. Quality control for retinal OCT in multiple sclerosis: validation of the OSCAR-IB criteria. Mult. Scler. J. 21 (2), 163–170. https://doi.org/10.1177/1352458514538110.

De Stefano, N., Stromillo, M.L., Giorgio, A., et al., 2015. Establishing pathological cut-offs of brain atrophy rates in multiple sclerosis. J. Neurol. Neurosurg. Psychiatry. https://doi.org/10.1136/jnnp-2014-309903. Published online April 22jnnp-2014-309903.

De Stefano, N., Arnold, D.L., 2015. Towards a better understanding of pseudoatrophy in the brain of multiple sclerosis patients. Mult. Scler. J. 21 (6), 675–676. https://doi.org/10.1177/1352458514564494.

Gordon-Lipkin, E., Chodkowski, B., Reich, D.S., et al., 2007. Retinal nerve fiber layer is associated with brain atrophy in multiple sclerosis. Neurology 69 (16), 1603–1609. https://doi.org/10.1212/01.wnl.0000295995.46586.ae.

Caverzasi, E., Papinutto, N., Cordano, C., et al., 2023. MWF of the corpus callosum is a robust measure of remyelination: results from the ReBUILD trial. Proc. Natl. Acad. Sci. 120 (20), e2217635120. https://doi.org/10.1073/pnas.2217635120.

Further reading

Patti, F., Visconti, A., Capacchione, A., Roy, S., Trojano, M., 2020. on behalf of the CLARINET-MS Study Group. Long-term effectiveness in patients previously treated with cladribine tablets: a real-world analysis of the Italian multiple sclerosis registry (CLARINET-MS). Ther. Adv. Neurol. Disord. 13. https://doi.org/10.1177/1756286420922685, 175628642092268.